

# Structural, optical and photoelectron spectroscopic studies of nano/micro ZnO: Cd rods synthesized via sol-gel route

U. N. Maiti · P. K. Ghosh · Sk. F. Ahmed · M. K. Mitra ·  
K. K. Chattopadhyay

Received: 25 March 2006 / Accepted: 14 June 2006 / Published online: 6 October 2006  
© Springer Science + Business Media, LLC 2006

**Abstract** Thin films of cadmium doped zinc oxide rod like microstructure have been synthesized by a very simple sol-gel dip coating technique. Sols were prepared from hydrated zinc oxide precursor and 2-methoxyethanol solvent with monoethanolamine as a sol stabilizer. XRD pattern confirmed the hexagonal wurtzite structure of the deposited ZnO films. Surface morphologies of the films have been studied by a scanning electron microscope and an atomic force microscope, which confirmed that the films are composed of densely packed randomly oriented nano/submicron rods with diameter in the range 300–400 nm having various lengths. We proposed a possible growth mechanism for this rodlike structure. X-ray photoelectron spectroscopic study was used to determine the binding energies and the Zn 2p<sub>3/2</sub>, Cd 3d<sub>5</sub> and O 1s peaks in the XPS spectra were located at 1021.08 eV, 404.6 eV and 529.8 eV respectively, which confirmed the Cd doping in ZnO. Cadmium content in the film was estimated both from energy dispersive X-ray analysis and XPS measurement. Band gap energy determined from optical transmittance spectra systematically varied from 3.28 eV to 3.15 eV for 0% to 5.6% of Cd doping. Urbach parameter determined from the band tail of the transmittance spectra showed that it increased with doping percentage and this parameter for a fixed cadmium doping level decreased with increase of temperature.

**Keywords** ZnO · Cd doping · Nano-micro rod · SEM · AFM · XPS · Optical property

## 1 Introduction

Zinc oxide possesses a unique position among the materials owing to its superior and diverse properties such as piezoelectricity, chemical stability, biocompatibility, optical transparency in the visible region and high voltage-current nonlinearity etc. [1]. These properties of ZnO impose its immense potential in different applications such as in solar cells [2–5], transparent electrodes [6–8], blue/UV light emitter device [9], gas sensor [10], transducer [11] etc. An important step in order to design ZnO-based devices is the realization of band gap engineering to create barrier layers and quantum wells in device heterostructures. Cd incorporation into ZnO serves the purpose of band gap narrowing efficiently because of the smaller band gap of CdO (2.3 eV) as compared to ZnO (3.32 eV), keeping the crystalline structure and lattice parameter close to ZnO. Furthermore it is now well known that increase in surface to volume ratio has great effect on material properties. Recently, 1-D structure of Cd doped ZnO draws attention of the researchers. Very recently, resistance and humidity sensing property of Cd-doped ZnO nanowires have been reported [12] which take advantage of a large surface to volume ratio of nanowires.

In recent time there are many reports of Cd doped ZnO either in thin film or nanostructured form with varying amount of Cd incorporation. Almost all these reports used complicated physical processes such as pulsed laser deposition (PLD) [13], metal-organic vapor phase epitaxy (MOVPE) [14], vapor-liquid-solid (VLS) [15] etc. Therefore, it is practically important to develop a simpler method for the preparation of Cd doped ZnO through chemical route.

---

U. N. Maiti · P. K. Ghosh · S. F. Ahmed ·  
K. K. Chattopadhyay (✉)  
Department of Physics,  
Thin Films and Nanoscience Laboratory, Jadavpur University,  
Kolkata 700 032, India  
e-mail: kalyan.chattopadhyay@yahoo.com

M. K. Mitra · K. K. Chattopadhyay  
Nanoscience and Technology Center, Jadavpur University,  
Kolkata 700 032, India

Reports of cadmium doped zinc oxide synthesized through chemical routes are rare. Only Choi et al. [16] reported sol-gel derived  $Zn_xCd_{1-x}O$  thin film but the surface morphology of the films has not been reported by them.

Sol-gel process has many advantages such as an easier composition control, better homogeneity, low processing temperature, lower cost, easier fabrication of large area films, possibility of using high purity starting materials and having an easy coating process of large and complex shaped substrates. In this paper we report successful synthesis of quasi one-dimensional Cd doped ZnO nano/submicro structured thin film via a very simple route which is similar as reported by our group for the fabrication of undoped ZnO nano/micro fibrous thin film [17]. Literature survey reveals that there is no report of Cd doped 1-D structured thin film by sol-gel dip coating technique. In addition to the simplicity of the technique the fibre growth parallel to the substrate should give a greater mechanical stability to the films as compared to films with vertical nanowires grown by vapor phase techniques without much sacrificing surface to volume ratio. Mechanical stability is significantly important to integrate these 1-D structures into devices because mechanical failure of these nanostructures may lead to malfunction or even fatal failure of the entire devices.

## 2 Experimental

### 2.1 Synthesis

The precursors for the synthesis of Cd doped 1-D nanostructured thin films were analytical grade zinc acetate dihydrate (Sigma-Aldrich, 99.99%), 2-methoxyethanol ( $C_3H_8O_2$ ) and monoethanolamine. Monoethanolamine was added to the zinc acetate solution as a stabilizer and the molar ratio of MEA to Zn ion was maintained at unity. Cd doping was achieved by the introduction of appropriate amount of cadmium acetate dihydrate ( $Cd(CH_3COO)_2 \cdot 2H_2O$ , Sigma-Aldrich 99.99%). In the process of doping Cd concentration was varied from 0% to 6% in molar percentage. A solution containing 0.016 mol of zinc acetate, cadmium acetate (0%–6%), 25 ml 2-methoxyethanol and monoethanolamine ( $[MEA]/[Zn^{2+}] = 1$ ) was vigorously stirred for 1 h with a magnetic stirrer, keeping the temperature of the solution at 348 K. Then, the solution was aged for 2 h to obtain the required sol. The films were deposited on normal sodalime glass substrate (Blue Star, India) by dip-coating technique. Microscopic glass slide substrates were cleaned prior to dipping. Glass slides were at first washed thoroughly with mild detergent then boiled for 30 min in distilled water and ultrasonicated for 15 min in acetone. Finally, the substrates were degreased in ethanol vapour. These glass slides were dipped into and withdrawn vertically slowly (8 cm/min.) from the

solution under ambient condition (temperature 297 K; humidity 55%). After each dip-coating, the substrates were heated at 423 K for 10 min, this process from coating to drying was continued for 6 times. Finally, the films coated on both sides of the substrate were heated at 673 K for 1 h in open-air furnace.

### 2.2 Characterization

After synthesizing the films, their structural, compositional, X-ray photoelectron spectroscopy (XPS) and optical characterizations were performed. X-ray diffraction patterns were recorded by an X-ray diffractometer (Bruker D8 Advance) in the  $2\theta$  range  $20\text{--}70^\circ$  using  $Cu K_\alpha$  radiation with wavelength  $\lambda = 0.15406$  nm operating at 40 kV, 40 mA. The surface morphology of the thin films was studied by a scanning electron microscope (SEM, JEOL-JSM-6360) and an atomic force microscope (AFM, NT MDT, Solver pro). The film compositions were determined by energy dispersive X-ray analysis (EDX, Oxford, model-7582) and XPS (HSA-3500 analyser SPECS, Germany). UV-Vis-NIR spectrophotometric measurements were performed by using a spectrophotometer (Shimadzu UV-3101PC) at room temperature. The spectra were recorded by taking a similar glass as a reference and hence the transmission due to the film only was obtained. The information about binding energies of different electronic states has been obtained by XPS.

## 3 Results and discussion

### 3.1 XRD study

Figure 1 shows the XRD patterns of as grown ZnO and 6% Cd doped ZnO thin films. Analysis of the XRD patterns for all the samples revealed that they are mono-phasic with

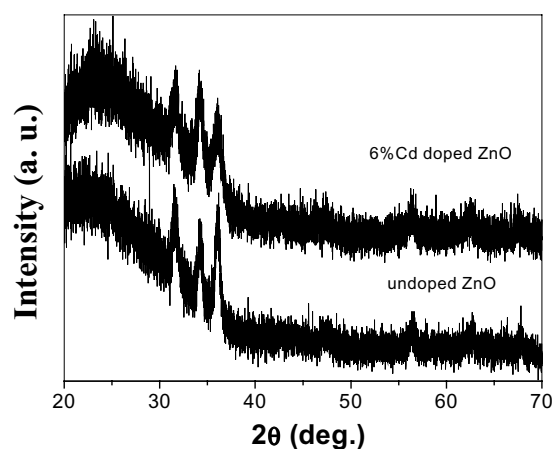


**Fig. 1** XRD pattern of Cd doped ZnO nano/submicro rod thin film on glass substrate

good crystallinity, all the appeared peaks can be indexed to the hexagonal wurtzite structure of ZnO with lattice constants  $a = 3.24 \text{ \AA}$  and  $c = 5.20 \text{ \AA}$  respectively. No secondary phases corresponding to oxides of cadmium, metallic cadmium or zinc metal cluster were observed, which suggest Cd incorporation into ZnO lattice. No significant changes in the lattice parameter with cadmium doping was observed, this is due to the fact that ionic radius of  $\text{Cd}^{2+}$  ( $0.74 \text{ \AA}$ ) is very close to that of  $\text{Zn}^{2+}$  ( $0.60 \text{ \AA}$ ) [15]. Broadening of the XRD peaks in the nano/submicro structured films occurred due to the small size of the crystallites and also due to strain developed in it. The length of coherence in the grains was estimated from the well-known Scherrer's relation corresponding to the broadening of the XRD peaks and it came out to be  $\sim 8 \text{ nm}$ .

### 3.2 Compositional analysis

Compositional analysis of the films was carried out by energy dispersive X-ray analysis. The dopant (Cd) concentration in the starting solution was varied from 0%–6% and then expected Cd/Zn ratio was = 0.00–0.06 in the film. We actually obtained from EDX, the Cd/Zn ratios in the range 0.000–0.056, compositional analysis from XPS also supported this results.

### 3.3 SEM studies

Scanning electron microscope (SEM) image shown in Fig. 2A shows a general view of the morphology of Cd doped ZnO thin film synthesized on glass substrate. High density of closely packed nano/submicro rods over a large area is clearly seen in the micrograph. Typical length of the rods varies from few microns to few hundred microns and diameter 300–400 nm. Generally, the growth of the 1-D structure is driven in one of the possible favored directions. In the present case, the growth of the rods was found to occur in the horizontal direction as shown in Fig. 2A.

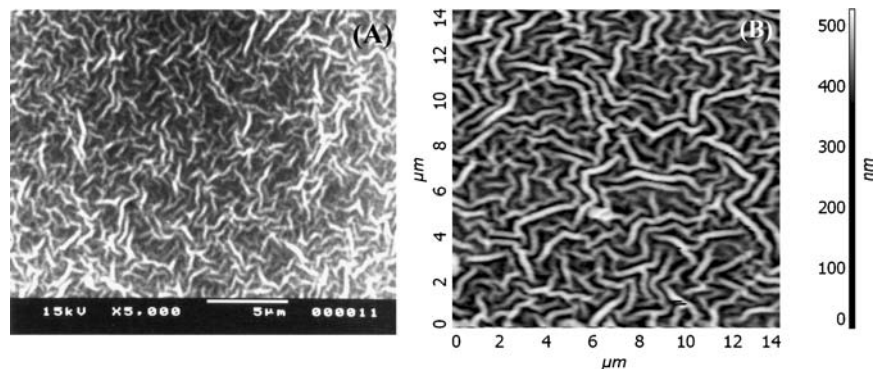
### 3.4 AFM study

AFM studies were also performed for observing the surface morphology of the films. Figure 2B shows the top-view image of the 6% Cd doped ZnO nano/submicro-structured thin film. It is evident from the figure that the film consists mainly of closely packed and randomly distributed rods of various lengths with few voids. The average diameter of the rods, measured from this figure is of the order of 400 nm which is same as obtained from SEM studies. We observed that with variation in doping level no significant structural change occurred.

### 3.5 XPS study

Incorporation of Cd into the ZnO lattice is also characterized by XPS measurement. XPS spectra have been charged corrected to the adventitious C 1s peak at 284.2 eV binding energy. The core levels of Zn 2p, Cd 3d5, and O 1s peaks were observed. Figure 3A to C shows the XPS spectra corresponding to Zn 2p<sub>3/2</sub>, O 1s and Cd 3d5 peaks respectively. The binding energies of the Zn 2p<sub>3/2</sub> and O 1s peaks are located at 1021.9 eV and at about 530 eV respectively [18]. The occurrence of the peaks corresponding to the binding energies of Zn 2p<sub>3/2</sub> (1021.08 eV) and O 1s (529.8 eV) respectively clearly show the formation of zinc oxide. The asymmetry in the 1s peak resulted from the formation of O–H bond [19]. The formation of O–H bond resulted from the hydroxylation of the film surface when exposed to air. The energy of Cd 3d5 level in CdO is 403 eV [20]. Occurrence of the peak at 404.6 eV indicates the absence of CdO phase in the sample. The chemical shifts of the peaks confirmed that Cd is really doped into ZnO. The asymmetry in the peak corresponding to Cd 3d5 is due to superposition of the two peaks corresponding to Cd 3d5/2 and Cd 3d since energy difference between these peaks is very small.

**Fig. 2** (A). SEM image for 6% Cd doped ZnO thin film. (B). A typical top-view AFM image of 6% Cd doped film



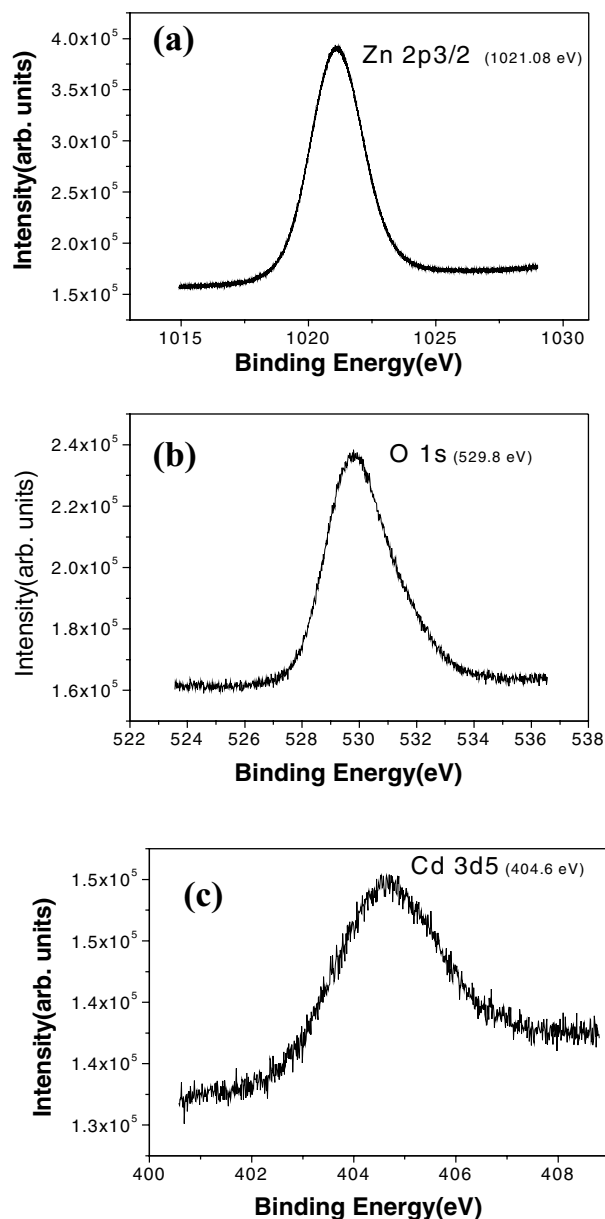


**Fig. 3** (a) XPS spectra corresponding to Zn 2p<sub>3/2</sub> (b) XPS spectra corresponding to O1s and (c) XPS spectra corresponding to Cd 3d<sub>5</sub>

### 3.6 Optical absorption measurement

Optical transmittance (T) of the films is plotted in the Fig. 4a as a function of wavelength in the wavelength range 300–800 nm. The transmittance spectra were measured by taking a similar glass as a reference and hence the spectra were from the films only. All the films exhibits more than 80% transmittance in the visible wavelength region and sharp ultraviolet absorption edge corresponding to undoped film suffers significant red shift with the increase of cadmium content. The sharp fall of the optical transmittance spectra of the films is due to the onset of the fun-

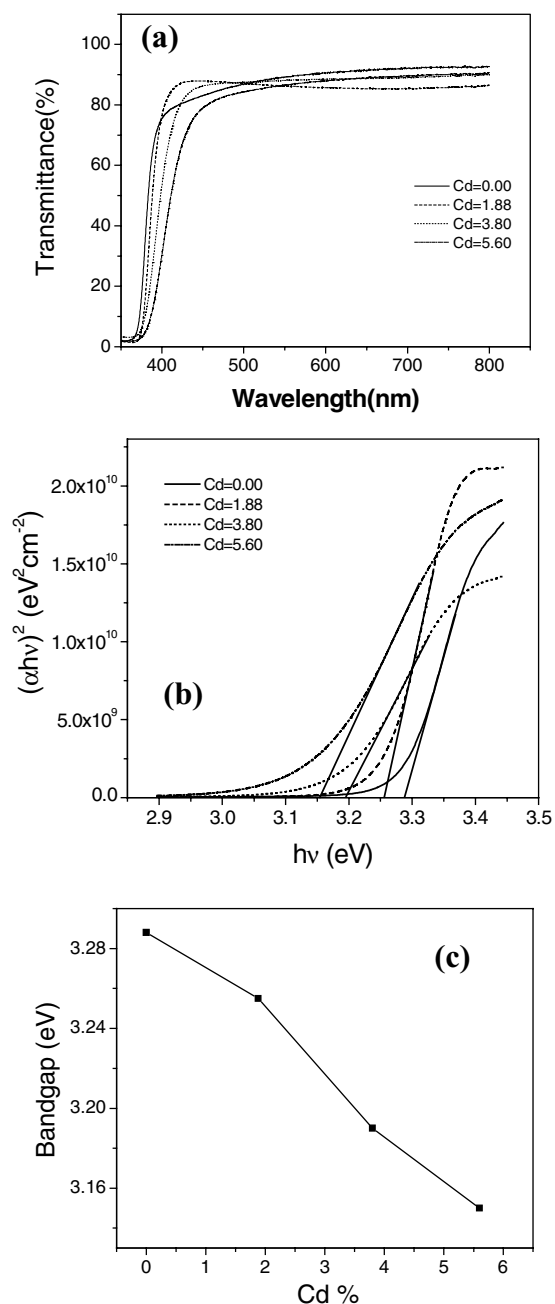


**Fig. 4** (a) Transmittance spectra of Cd doped ZnO microrods for different doping level (b) Plot to determine the direct band gap for different doping percentage and (c) Variation of bandgap energy with cadmium doping

damental absorption. The measured transmittance was converted into the absorption coefficient  $\alpha$ , using the relationship  $\alpha(\lambda) = 1/d[\ln(1/T)]$  where  $d$  is the film thickness, which was determined from cross-sectional SEM image (not shown here) to be  $\sim 900$  nm.

The energy gap ( $E_g$ ) can be estimated by assuming direct transition between conduction band and valance bands. The-ory of optical absorption gives the relationship between the

absorption coefficients  $\alpha$  and the photon energy  $h\nu$  for direct allowed transition as,

$$(\alpha h\nu)^2 = A(h\nu - E_g)$$

Where A is a function of index of refraction and hole/electron effective masses [21]. The direct band gap is determined using this equation when straight portion of the  $(\alpha h\nu)^2$  against  $h\nu$  plot is extrapolated to intersect the energy axis at  $\alpha = 0$ . Plot of  $(\alpha h\nu)^2$  against  $h\nu$  for undoped and cadmium doped microstructured ZnO films is shown in Fig. 4b. The variation of the band gap with cadmium content (x) is given in Fig. 4c. It is seen from Fig. 4c that with the increase of cadmium doping level bandgap decreases, this decrease is accounted for the fact that bandgap of CdO (bulk value 2.23 eV) is less than that of ZnO (bulk value 3.32 eV). The absorption coefficient  $\alpha$  near the band edge in the energy region  $h\nu < E_g$  empirically follows the exponential law i.e. Urbach tail is expressed by

$$\alpha(h\nu) = \alpha_0 \exp(h\nu/E_0)$$

where  $\alpha_0$  is a constant and  $E_0$  is an empirical parameter weakly depended on temperature and describing the width of the localized states in the bandgap, but not the energy position of the localized states. Several factors are responsible for Urbach band tail in semiconductor such as carrier-impurity interaction, carrier-phonon interaction, structural disorder [22] etc. Basically this parameter includes the effects of all possible defects [23].  $E_0$  values for different doping level were estimated from the slopes of the linear plot of  $\ln\alpha$  against  $h\nu$  as shown in Fig. 5a and is given in the Table 1. Urbach parameter( $E_0$ ) for undoped film is very much similar as reported by Aghamalyan et al. [24] for electron beam evaporated ZnO films. Increase of  $E_0$  with doping indicates that defect increases in the film with Cd incorporation.

Urbach paramater for the 5.6% doped films deposited on glass substrates at final annealing temperatures 673 K and 773 K are given in Fig. 5b. Analyzing these plots we observe that Urbach parameter decreases with increase of final annealing temperature which is due to smaller structural disorder at higher annealing temperature. This reflects the facts that at higher annealing temperature recrystallization of the clusters formed after drying is better.

**Table 1** Variation of Urbach parameter with doping percentage

Cd doping percentage (%)	Urbach parameter $E_0$ (meV)
0	73.8
2	75.05
4	123.28
6	154.94

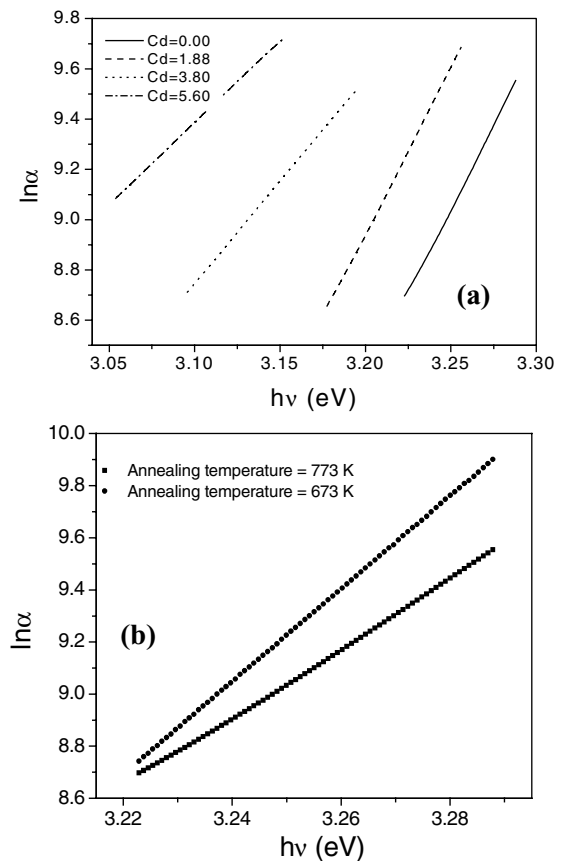


**Fig. 5** (a) Plot to determine Urbach parameter for different doping percentage (b) Urbach parameter for 6% doped ZnO film with final annealing temperatures 673 K and 773 K respectively

Although for complete understanding of the growth mechanism needs more work but we propose the following mechanism. Since no external source of precursors is admitted during the annealing processes, the possibility of growth of microstructures in the vertical direction can be ruled out. During successive coating and subsequent drying processes some roughness generates in the film which act as nucleation centers and the sol tends to deposit more over the rough area rather than the smooth region, as it is well known that defects acts as nucleation centers. This process continues during each drying process so that the films are composed of clusters. It is believed that the monoethanolamine ( $C_2H_7NO$ ) molecule, used in the precursor solution played the role of a director for the growth of rods, and without using it, no growth of ZnO rods were observed. During the final annealing at 673 K the clusters coalesce and recrystallize to form the final randomly distributed polycrystalline rod-like structure. M. Ohyama et al.[25] also reported ZnO thin film preparation by a nearly similar technique without obtaining rod like morphology. Although the reason of not obtaining a rod like morphology by them is not fully clear to us, possibly the duration of heat treatment along with heating and cooling rate

which are very important in obtaining the rod like morphology were different in their synthesis method compared to us.

#### 4 Conclusion

Fabrication of cadmium doped ZnO microstructured thin film was achieved through a very simple sol-gel dip coating technique. SEM and AFM images showed the films consist of densely packed nano/submicro rods. XRD spectra showed that the films are of hexagonal wurtzite structure. XPS spectra confirmed that Cd is doped into ZnO. With increase of Cd doping bandgap decreases and the Urbach parameter, which gives the width of the localized states in the bandgap, also increases. It is observed that the diameters of the rods are smaller than compared to our previous report of ZnO nano/submicro rods. We believe that proper variation of deposition parameters would give thinner rods. Due to large variation of the bandgap with small doping percentage, they can be used as an excellent candidate for the preparation of quantum wells, superlattices and other configurations that involved bandgap engineering. Cd doped ZnO microstructures offers potential application as humidity sensors due to its large surface to volume ratio.

**Acknowledgement** One of us (UNM) wishes to thank Council of Scientific and Industrial Research (CSIR), Govt. of India, for awarding him a junior research fellowship (JRF) during the execution of the work. The authors wish to thank University Grants Commission (UGC), Govt. of India, for financial assistance through 'University with potential for excellence programme'.

#### References

1. Look DC (2001) *Mater Sci Eng B* 80:383
2. Lee C, Lim K, Song J (1996) *Solar Energy Mater Solar Cells* 43:37
3. Bahadur L, Hamdani M, Koenig JF, Chartier P (1986) *Solar Energy Mater* 14:107
4. Negami T, Hashimoto Y, Nishiwaki S (2001) *Solar Energy Mater Solar Cells* 67:331
5. Matsubara K, Fons P, Iwata K, Yamada A, Sakurai K, Tampo H, Niki S (2003) *Thin Solid Films* 431:369
6. Ohya Y, Ueda M, Takahashi Y (1996) *Jpn J Appl Phys* 35:4738
7. Natsume Y, Sakata H (2000) *Thin Solid Films* 372:30
8. Paul GK, Bandyopadhyay S, Sen SK (2002) *Phys Status Solidi A* 191:509
9. Look DC, Reynolds DC, Litton CW, Jones RL, Eason DB, Cantwell G (2002) *Appl Phys Lett* 81:1830
10. Wang X, Carey WP, Yee S (1995) *Sensors Actuators B* 28:63
11. Srivastava JK, Agrawal L, Bhattacharyya B (1989) *J Electrochem Soc* 11:3414
12. Wan Q, Li QH, Chen YJ, Wang TH, He XL, Gao XG, Li JP (2004) *Appl Phys Lett* 84:3085
13. Makino T, Segawa Y, Kawasaki M, Ohtomo A, Shiroki R, Tamura K, Yasuda T, Koinuma H (2001) *Appl Phys Lett* 78:1237
14. Gruber Th, Kirchner C, Kling R, Reuss F, Waag A, Bertram F, Forster D, Christen J, Schreck M (2003) *Appl Phys Lett* 83:3290
15. Wang FZ, Ye ZZ, Ma DW, Zhu LP, Zhuge F, He HP (2005) *Appl Phys Lett* 87:143101
16. Choi Y-S, Lee C-G, Cho SM (1996) *Thin Solid Films* 289:153
17. Maity R, Das S, Mitra MK, Chattopadhyay KK (2005) *Physica E* 25:605
18. Jing L, Xu Z, Sun X, Shang J, Cai W (2001) *Appl Surface Sci* 180:308
19. Gu ZB, Yuan CS, Lu MH, Wang Z, Wu D, Zhang ST, Zhu SN, Zhu YY, Chen YF (2005) *J Appl Phys* 98:053908
20. Bose DN, Hedge MS, Basu S, Mandal KC (1989) *Semicond Sci Technol* 4:866
21. Pankove JI (1971) *Optical processes in semiconductors*. Prentice-Hall, Englewood Cliffs, NJ
22. Chen NB, ZWu H, Qiu DJ, Xu TN, Chen J, Shen WZ (2004) *J Phys: Condens Matter* 16:2973
23. Srikant V, Clarke DR (1997) *J Appl Phys* 81:6357
24. Aghamalyan NR, Gambaryan IA, Goulanian E Kh, Hovsepian RK, Kostanyan RB, Petrosyan SI, Vardanyan ES, Zerrouk AF (2003) *Semicond Sci Technol* 18:525
25. Ohyama M, Kozuka H, Yoko T (1997) *Thin Solid Films* 306:78